

SS-traveltime parameters from PP- and PS-reflections

Bjørn Ursin*, Martin Tygel†, and Einar Iversen‡

* Dept. of Petroleum Eng. and Appl. Geophysics, NTNU, S.P. Andersensvei 15A, NO-7491 Trondheim, Norway

† Dept. of Applied Math., IMECC-UNICAMP, CP 6065, 13083-859 Campinas (SP), Brazil

‡ NORSAR, P.O. Box 53, 2027 Kjeller, Norway

Copyright 2009, SBGf - Sociedade Brasileira de Geofísica

This paper was prepared for presentation at the 11th International Congress of The Brazilian Geophysical Society held in Salvador, Brazil, August 24-28, 2009.

Contents of this paper was reviewed by The Technical Committee of The 11th International Congress of The Brazilian Geophysical Society and does not necessarily represents any position of the SBGf, its officers or members. Electronic reproduction, or storage of any part of this paper for commercial purposes without the written consent of The Brazilian Geophysical Society is prohibited.

Abstract

SS-wave traveltimes can be derived from PP- and PS-wave data with the previously derived “PP + PS=SS” method. We extend this method as follows: 1) The previous requirement that sources and receivers need to be located on a common acquisition surface is removed, which makes the method directly applicable to PS-waves recorded on the ocean bottom and PP-waves recorded at the ocean surface. 2) By using the concept and properties of surface-to-surface propagator matrices, the second-order traveltimes of the SS-waves are obtained. In the same way as for the original “PP+PS=SS” method, the proposed extension is valid for arbitrary anisotropic media. The propagator matrix and geometric spreading of an SS-wave reflected at a given point on a target reflector are explicitly obtained from the propagators of the PP- and PS-waves reflected at the same point. These additional parameters provided by the extended “PP+PS=SS” method can be used for a partial reconstruction of the SS-wave amplitude as well as for tomographic estimation of the elastic velocity model. A full simulation of the SS-wave, which includes reflection and transmission coefficients, cannot be directly obtained from the knowledge of PP- and PS-amplitudes.

Introduction

Present acquisition, e.g., from ocean bottom and land seismics, rely on P-wave source excitations giving rise essentially to PP- and PS-wave field data. In this way, shear-wave velocities can only be derived from converted PS-waves included in the data. This fact has been responsible for the high interest in the development of processing/imaging methodologies and tools that are able to extend the classical ones available for non-converted waves.

In principle, processing of SS-waves, if available in the seismic data, would parallel the one routinely carried out for PP-waves to provide corresponding S-wave information. In the near-offset situation, normal moveout (NMO) velocities or normal-incidence-point (NIP) wave curvatures (Hubral, 1983) can be found from a conventional (time-domain) velocity analysis. NMO-velocities correspond to second-order derivatives of non-converted wave traveltimes, assumed to

be of type PP or SS. In this way, one avoids dedicated traveltimes processing to obtain these velocities. Together with the traveltimes and slopes, the NIP-wave curvatures can be applied to tomographic inversion in isotropic models for the corresponding P- and S-wave velocity fields, [see, e.g., Iversen and Gjøystdal (1984) and Duvoneck (2004) for the PP-situation].

Grechka and Tsvankin (2002) introduced a method to (kinematically) simulate SS-reflections by means of a suitable combination of PP- and PS-reflections. More specifically, the method, referred to as “PP+PS=SS” method, selects identified traveltimes and slopes of PP- and PS-reflections of the same reflector to produce the corresponding SS-reflection traveltimes and slopes from that reflector.

The obtained SS-reflections can be incorporated to the original seismic volume as SS-reflection data and processed in the same way as for PP-waves. The PP+PS=SS methodology has been used in Foss et al. (2005) for depth-consistent tomography of PP- and PS-reflections. For a few key reflectors, the zero-offset PP- and PS-traveltimes were used to estimate the SS-reflection times. These were then employed together with the PP traveltimes for reflector co-depthing.

A natural question is whether the knowledge of the second-order traveltimes derivatives of PP- and PS-waves, as provided by their ray-propagator matrices, leads to the ray-propagator matrix of the corresponding SS-wave. In this paper, we show that the answer to this question is affirmative. By using the “algebra” of ray-propagator matrices, as described in, e.g., Červený (2001), an explicit relationship between the involved PP-, PS- and SS-ray-propagator matrices is achieved. By examining the relationships that exist between the coefficients of the second-order Taylor expansion of traveltimes and the submatrix components of the PP-, PS- and SS- ray-propagator matrices, we see that the new results provide the second-order derivatives of SS-traveltime thus extending the counterpart zero- and first-order derivatives provided by the original “PP+PS=SS” method of Grechka and Tsvankin (2002). Moreover, the simple assumption that sources and receivers are located on a common planar acquisition surface is removed, which makes the method directly applicable to PS-waves recorded on the ocean bottom and PP-waves recorded at the ocean surface.

A main application of the proposed extension of the “PP+PS=SS” method is that it opens the way for tomographic reconstruction of the elastic velocity model using, besides first-order derivatives (slopes), also second-order

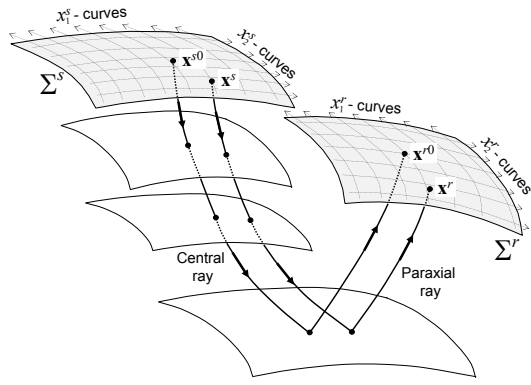


Figure 1: Central and paraxial rays from anterior, Σ^s , to posterior, Σ^r , surfaces. Points x^{s0} and x^s are central and paraxial sources specified in orthogonal curvilinear coordinates on the anterior surface. Points x^{r0} and x^r are corresponding central and paraxial receivers specified on the posterior surface.

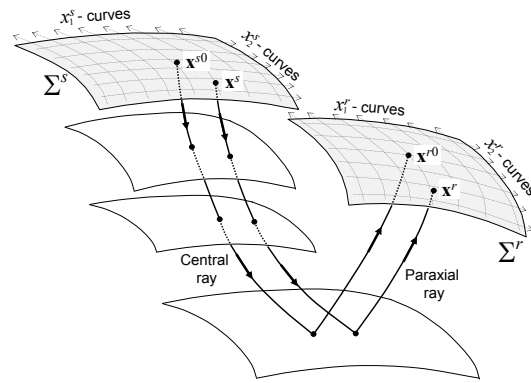


Figure 2: One PP- and two PS-reflections with a common reflection point, y . PP-reflection is from x^a to x^d . PS-reflections are from x^a to x^c and from x^d to x^b , respectively. The unit normal to the reflector at y is \mathbf{n} .

derivatives (curvatures) of SS-traveltimes. The method makes it possible to perform a quite accurate prediction of the SS-wave traveltime parameters and an approximate prediction of the SS-wave amplitude. It can thus be regarded as a modeling approach, with the great advantage that it requires very limited knowledge of the velocity model.

The present approach does not permit, however, to obtain a full simulation of the SS-wave, including the effects of reflection and transmission coefficients, based only on observed PP- and PS-wave amplitudes.

Surface-to-surface traveltime approximations

The formulation and main derivations of the extended “PP+PS=SS” method proposed here can be conveniently described using the concepts and basic properties of surface-to-surface propagator matrices. These are briefly

summarized below, following Červený (2001) as a main reference. For the zero-offset situation, the papers Bortfeld (1989) and Iversen (2006) are to be cited. Specific treatment of traveltime is given in Schleicher et al. (1993).

Figure 1 shows a fixed (central) ray that connects a (central) source point at an *anterior surface*, Σ^s , to a (central) receiver point at a *posterior surface*, Σ^r . The central ray traverses a medium consisting of inhomogeneous anisotropic layers bounded by curved interfaces. We assume that both anterior and posterior surfaces, as well as all interfaces and also the medium within the layers are sufficiently smooth so that wave propagation is well described by zero-order ray theory. Orthogonal curvilinear coordinates (x_1^s, x_2^s, x_3^s) and (x_1^r, x_2^r, x_3^r) are associated with, respectively, the anterior and posterior surfaces, in such a way that x_3^s and x_3^r are both constants (e.g., equal zero) along these surfaces. For the first two components of the curvilinear coordinates we use the vector/matrix notations $\mathbf{x}^s = (x_1^s, x_2^s)^T$ and $\mathbf{x}^r = (x_1^r, x_2^r)^T$, where superscript T means transposition. To avoid unnecessary complication of terminology, we have not introduced a specific, parallel, notation for points in 3D space. This means that we refer to such a point as, e.g., “the point \mathbf{x}^s ”, although, strictly speaking, the vector \mathbf{x}^s specifies only two (curvilinear) coordinates of the point under consideration.

Figure 1 finally shows an arbitrary paraxial ray that starts on surface Σ^s and ends on surface Σ^r . By definition, the paraxial ray has the same wavemode signature and a sufficiently close trajectory to the central ray. Under the present assumptions of smooth model parameters and interfaces, any such paraxial ray is completely determined by the differences in the curvilinear coordinates of the initial and end points relative to the central source and receiver points, respectively. Attached to the central ray, the 4×4 surface-to-surface ray propagator matrix has the form

$$\mathbf{T} = \begin{pmatrix} \mathbf{A} & \mathbf{B} \\ \mathbf{C} & \mathbf{D} \end{pmatrix}, \quad (1)$$

where \mathbf{A} , \mathbf{B} , \mathbf{C} , and \mathbf{D} are 2×2 constant submatrices. Matrix \mathbf{T} incorporates the dynamic quantities (second-order derivatives of traveltime) of the central ray, as well as the properties of the anterior and posterior surfaces and those of the medium in which the central ray propagates. The propagator matrix expresses, then, the first-order (linear) relationship between the relative differences with respect to the central ray of the projections of the position and slowness vectors onto the anterior and posterior surfaces. The propagator matrix satisfies the relationships

$$\mathbf{T}^{-1} = \begin{pmatrix} \mathbf{D}^T & -\mathbf{B}^T \\ -\mathbf{C}^T & \mathbf{A}^T \end{pmatrix}, \quad \mathbf{T}^{rev} = \begin{pmatrix} \mathbf{D}^T & \mathbf{B}^T \\ \mathbf{C}^T & \mathbf{A}^T \end{pmatrix}, \quad (2)$$

which are natural consequences of ray theory. In equation 2 the operation signified by the superscript *rev* implies that the resulting propagator matrix on the left-hand side corresponds to the reverse ray direction, i.e., the direction from \mathbf{x}^r to \mathbf{x}^s rather than from \mathbf{x}^s to \mathbf{x}^r . From equation 2 we obtain $\mathbf{C} = (\mathbf{D}\mathbf{A}^T - \mathbf{I})\mathbf{B}^{-T}$, where \mathbf{I} is the 2×2 identity matrix and the superscript $-T$ denotes the transpose of the inverse matrix.

The propagator matrix satisfies also the important *continuation property* or *chain rule*, which states that, if $\mathbf{T}(\mathbf{x}^b, \mathbf{x}^a)$ is the propagator matrix of a ray that connects \mathbf{x}^a to \mathbf{x}^b , and for a given intermediate point, \mathbf{x}^c , along the ray, $\mathbf{T}(\mathbf{x}^c, \mathbf{x}^a)$ and $\mathbf{T}(\mathbf{x}^b, \mathbf{x}^c)$ are the propagator matrices for the rays segments from \mathbf{x}^a to \mathbf{x}^c and from \mathbf{x}^c to \mathbf{x}^b , respectively, then

$$\mathbf{T}(\mathbf{x}^b, \mathbf{x}^a) = \mathbf{T}(\mathbf{x}^b, \mathbf{x}^c) \mathbf{T}(\mathbf{x}^c, \mathbf{x}^a). \quad (3)$$

The second-order Taylor expansion of traveltime of a paraxial ray in terms of its relative source and receiver coordinates is given by (see, e.g., Schleicher et al., 1993)

$$t(\mathbf{x}^r, \mathbf{x}^s) = t^0 + (\mathbf{p}^{r0})^T \Delta \mathbf{x}^r - (\mathbf{p}^{s0})^T \Delta \mathbf{x}^s (\Delta \mathbf{x}^r)^T \mathbf{M}^{rs} \Delta \mathbf{x}^s + \frac{1}{2} (\Delta \mathbf{x}^r)^T \mathbf{M}^{rr} \Delta \mathbf{x}^r + \frac{1}{2} (\Delta \mathbf{x}^s)^T \mathbf{M}^{ss} \Delta \mathbf{x}^s, \quad (4)$$

where $t^0 = t(\mathbf{x}^{s0}, \mathbf{x}^{r0})$ is the traveltime along the central ray and $\mathbf{p}^{s0} = (\partial t / \partial \mathbf{x}^s)$ and $\mathbf{p}^{r0} = (\partial t / \partial \mathbf{x}^r)$ are the coefficients of the linear (slowness) terms. Moreover, $(\partial^2 t / \partial \mathbf{x}^s \partial \mathbf{x}^r)$, $\mathbf{M}^{ss} = (\partial^2 t / \partial \mathbf{x}^s \partial \mathbf{x}^s)$ and $\mathbf{M}^{rr} = (\partial^2 t / \partial \mathbf{x}^r \partial \mathbf{x}^r)$ are the coefficients of the quadratic terms. All the derivatives are evaluated for $\mathbf{x}^s = \mathbf{x}^{s0}$ and $\mathbf{x}^r = \mathbf{x}^{r0}$. The symmetric matrix \mathbf{M}^{ss} is related to the wavefront curvatures at \mathbf{x}^{r0} for a point source at \mathbf{x}^{s0} , while the symmetric matrix \mathbf{M}^{rr} is related to the wavefront curvatures at \mathbf{x}^{s0} for a point source at \mathbf{x}^{r0} . Matrix \mathbf{M}^{rs} of second-order mixed derivatives is related to the relative geometric spreading.

The traveltime approximation in equation 4 has the same structure as the ones defined for paraxial rays with arbitrary 3D relative source and receiver coordinates (see, e.g., Ursin, 1982). By squaring equation 4 and retaining the terms up to second order only, we obtain the more commonly used Taylor series for traveltime squared. From the basics of Taylor series expansions, the approximation 4 is valid for "sufficiently small" arguments, \mathbf{x}^s and \mathbf{x}^r , meaning that paraxial rays should be "sufficiently close" to the central ray. A general quantification of the accuracy of the approximations is impossible, as it depends on the properties of the medium, basically smoothness of medium parameters and interfaces. In spite of their limited accuracy, Taylor approximations have been used with quite good success in seismic imaging. With the help of the propagator matrix, we have the important relationships

$$\mathbf{M}^{rr} = \mathbf{D}\mathbf{B}^{-1}, \quad \mathbf{M}^{ss} = \mathbf{B}^{-1}\mathbf{A} \quad \text{and} \quad \mathbf{M}^{rs} = -\mathbf{B}^{-1}. \quad (5)$$

From these, the matrix components, \mathbf{A} , \mathbf{B} , \mathbf{C} and \mathbf{D} , of the propagator matrix, \mathbf{T} , can be obtained. In the following, we assume that the traveltime Taylor series expansions are valid, and that the traveltime parameters, t^0 , \mathbf{p}^{s0} , \mathbf{p}^{r0} , \mathbf{M}^{rr} , \mathbf{M}^{rs} and \mathbf{M}^{ss} , can be estimated from the seismic data.

SS-TRAVELTIME PARAMETERS

We consider survey configurations with source and receiver points distributed on two surfaces, as follows: *Acquisition surface 1* (e.g., the ocean surface), denoted as Σ^1 , shall consist of source points for PP-reflected and PS-reflected waves and receiver points for PP-reflected waves. *Acquisition surface 2* (typically the ocean bottom), denoted as Σ^2 , consists of receiver points for PS-reflected waves. As a special case (land seismics) these two surfaces coincide. For the common situation in ocean bottom seismics

that the PP-reflected waves have actually been recorded on the ocean bottom (surface Σ^2), it will be necessary either to perform receiver-redatuming of the PP-reflected events to surface Σ^1 , or to perform source-redatuming of all PP- and PS-reflected events to surface Σ^2 .

With the above requirements on sources and receivers, we consider one PP-wave and two PS-waves for the same reflection point \mathbf{y} , as outlined in Figure 2. The slowness vectors and the normal vector, \mathbf{n} , of the reflecting interface at the point \mathbf{y} all lie in a common plane (Snell's law). The source and receiver points corresponding to the PP-reflection at \mathbf{y} are denoted, respectively, as \mathbf{x}^a and \mathbf{x}^d . Correspondingly, the receiver points of the two PS-waves reflected at \mathbf{y} are denoted \mathbf{x}^b and \mathbf{x}^c . As also shown in Figure 2, the PP-ray intersects surface Σ^2 at the points \mathbf{x}^α and \mathbf{x}^δ , respectively.

In the above perspective, the points \mathbf{x}^b and \mathbf{x}^c can be considered as virtual source and receiver points of an SS-wave reflected at the point \mathbf{y} . Moreover, for any given PP-wave source/receiver couple, $(\mathbf{x}^a, \mathbf{x}^d)$, the corresponding SS-wave virtual source/receiver couple, $(\mathbf{x}^b, \mathbf{x}^c)$, will be unknown. In order to determine $(\mathbf{x}^b, \mathbf{x}^c)$, we start by identifying a PP-reflection for the couple $(\mathbf{x}^a, \mathbf{x}^d)$ and estimate its traveltime parameters. Next, the PS-waves from \mathbf{x}^a to \mathbf{x}^c and from \mathbf{x}^d to \mathbf{x}^b are identified such that the slowness vectors of the P-waves at \mathbf{x}^a and \mathbf{x}^d are parallel to the corresponding PP-wave slowness vectors at the same points (Grechka and Tsvankin, 2002). The traveltime parameters for the two PS-waves are also estimated. It is then straightforward to show that the traveltime for the SS-wave satisfies the equation derived by Grechka and Tsvankin (2002) under the assumption of a common acquisition surface for all sources and receivers, namely,

$$t^{SS}(\mathbf{x}^c, \mathbf{x}^b) = t^{SP}(\mathbf{x}^c, \mathbf{x}^a) + t^{SP}(\mathbf{x}^b, \mathbf{x}^d) - t^{PP}(\mathbf{x}^d, \mathbf{x}^a). \quad (6)$$

Using the continuation property of the propagator matrix (see equation 3), the surface-to-surface ray propagators of PP- and PS-reflections are given by:

$$\begin{aligned} \mathbf{T}^{PP}(\mathbf{x}^d, \mathbf{x}^a) &= \mathbf{T}^P(\mathbf{x}^d, \mathbf{x}^\delta) \mathbf{T}^P(\mathbf{x}^\delta, \mathbf{y}) \mathbf{T}^P(\mathbf{y}, \mathbf{x}^\alpha) \mathbf{T}^P(\mathbf{x}^\alpha, \mathbf{x}^a), \\ \mathbf{T}^{SP}(\mathbf{x}^c, \mathbf{x}^a) &= \mathbf{T}^S(\mathbf{x}^c, \mathbf{y}) \mathbf{T}^P(\mathbf{y}, \mathbf{x}^\alpha) \mathbf{T}^P(\mathbf{x}^\alpha, \mathbf{x}^a), \\ \mathbf{T}^{SP}(\mathbf{x}^b, \mathbf{x}^d) &= \mathbf{T}^S(\mathbf{x}^b, \mathbf{y}) \mathbf{T}^P(\mathbf{y}, \mathbf{x}^\delta) \mathbf{T}^P(\mathbf{x}^\delta, \mathbf{x}^d). \end{aligned} \quad (7)$$

Here, the superscripts denotes the wavetypes and the indexing is from right to left (as in equation 6). For further use, we note that

$$\mathbf{T}^S(\mathbf{y}, \mathbf{x}^b) = [\mathbf{T}^P(\mathbf{x}^\delta, \mathbf{y})]^{-1} [\mathbf{T}^P(\mathbf{x}^d, \mathbf{x}^\delta)]^{-1} [\mathbf{T}^{SP}(\mathbf{x}^b, \mathbf{x}^d)]^{rev}, \quad (8)$$

where the inverse and reverse matrices are given in equation 2. Using the continuation property in equation 3, the SS-wave propagator matrix can be factored as

$$\mathbf{T}^{SS}(\mathbf{x}^c, \mathbf{x}^b) = \mathbf{T}^S(\mathbf{x}^c, \mathbf{y}) \mathbf{T}^S(\mathbf{y}, \mathbf{x}^b). \quad (9)$$

Then, by inserting equations 8 into equation 9 and after some algebra, it follows that the surface-to-surface ray propagator for the SS-wave from \mathbf{x}^b to \mathbf{x}^c is given by

$$\mathbf{T}^{SS}(\mathbf{x}^c, \mathbf{x}^b) = \mathbf{T}^{SP}(\mathbf{x}^c, \mathbf{x}^a) [\mathbf{T}^{PP}(\mathbf{x}^d, \mathbf{x}^a)]^{-1} [\mathbf{T}^{SP}(\mathbf{x}^b, \mathbf{x}^d)]^{rev}. \quad (10)$$

Equation 10 constitutes the main theoretical result of this paper. From the ray propagator matrix for the SS-wave we can compute the second-order traveltime parameters using equation 5.

SLOPE MATCHING BASED ON SECOND-ORDER TRAVELTIME DERIVATIVES

The extended “PP+PS=SS” method described above makes use of computed second derivatives of PP- and PS-wave traveltimes. This offers the possibility of using such derivatives to match slopes of PP- and PS-reflections.

Consider the problem of finding a root ξ of the nonlinear vector equation $f(\xi) = 0$ using an iteration technique of the Newton-Raphson type. Under the assumption of equal dimensionality of ξ and f , the inherent linearization of each iteration step yields the following update of ξ with respect to the current solution ξ^0 ,

$$\xi = \xi^0 - \left[\frac{\partial f}{\partial \xi^T}(\xi^0) \right]^{-1} f(\xi^0). \quad (11)$$

The slope matching consists of two independent steps, which collectively make use of equation 11. In the first step we consider a PS-wave for which the source point is located at x^a (Figure 2). The function f is defined by

$$f(\xi) = \frac{\partial t^{PP}}{\partial x^a}(x^d, x^a) - \frac{\partial t^{SP}}{\partial x^a}(\xi, x^a), \quad (12)$$

with the first derivatives given by

$$\frac{\partial f}{\partial \xi^T}(\xi) = \frac{\partial^2 t^{SP}}{\partial \xi \partial x^{aT}}(\xi, x^a) = -M^{rs}(\xi, x^a). \quad (13)$$

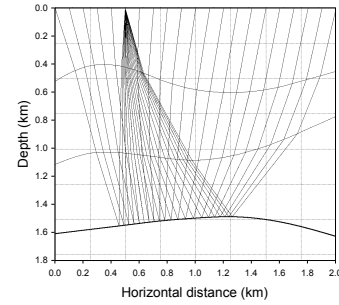
The matrix M^{rs} in equation 13 belongs to the PS-wave. We let the iteration process proceed until the criterion $f(\xi) = 0$ is satisfied, which yields the sought solution $\xi = x^c$. In the second step we consider another PS-wave, having x^d as its source point (Figure 2). The function f and its derivatives can now be specified by

$$f(\xi) = \frac{\partial t^{PP}}{\partial x^d}(x^a, x^d) - \frac{\partial t^{SP}}{\partial x^d}(\xi, x^d), \quad (14)$$

$$\frac{\partial f}{\partial \xi^T}(\xi) = \frac{\partial^2 t^{SP}}{\partial \xi \partial x^{dT}}(\xi, x^d) = -M^{rs}(\xi, x^d). \quad (15)$$

Again, the matrix M^{rs} belongs to the PS-wave. The output from this second iteration step is the solution $\xi = x^b$. Note especially that only one iterative slope-matching step is required in the normal-incidence situation. The slope matching procedure finds the (virtual) SS-wave source and receiver points x^c and x^d which correspond to the (real) source and receiver points for the recorded PP-waves. The convergence of this Newton-Raphson formulation is fast, required that the applied second-order traveltime derivatives are smooth functions. An alternative is to use a nonlinear inversion technique that does not require computation of the first derivatives of the function f (and thus the second derivatives of the traveltimes). Such techniques are generally slower, although more robust, than the Newton-Raphson approach.

(a)



(b)

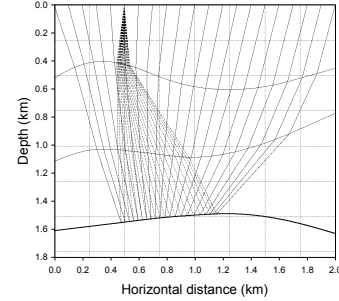


Figure 3: (a) PP-wave rays, (b) PS-rays

Numerical example

In this section we present a numerical example demonstrating the extended “PP+PS=SS” method. Our experiment is conducted with a model similar to the one used by Grechka and Tsvankin (2002). The model is two-dimensional and consists of three homogeneous VTI layers. The layers are separated by smoothly curved interfaces, which were generated by digitizing the interfaces plotted in Grechka and Tsvankin’s paper. For the latter reason, the models used by Grechka and Tsvankin (2002) and us are not exactly the same; however, in practice they can be considered equal. We consider quasi-P and quasi-SV wave types. Hence, in each layer the wave propagation is described by four parameters, specified using Thomsen’s (1986) representation:

- Top layer: $V_{P0} = 2.0$ km/s, $V_{S0} = 0.8$ km/s, $\epsilon = 0.20$, $\delta = 0.10$
- Middle layer: $V_{P0} = 2.5$ km/s, $V_{S0} = 1.25$ km/s, $\epsilon = 0.25$, $\delta = 0.05$
- Bottom layer: $V_{P0} = 3.0$ km/s, $V_{S0} = 1.8$ km/s, $\epsilon = 0.15$, $\delta = 0.10$

Traveltime “observations” corresponding to PP and PS reflections from the lowest interface of the bottom layer were generated using ray tracing. Figure 3 shows PP rays (a) and PS rays (b) for a common receiver at the horizontal coordinate $x = 0.5$ km. The corresponding traveltime observations for all source and receiver locations are shown, respectively, in Figure 4.

The (a), (b), and (c) subfigures constituting Figure 5 show the PP-, PS-, and SS-wave relative geometric spreading

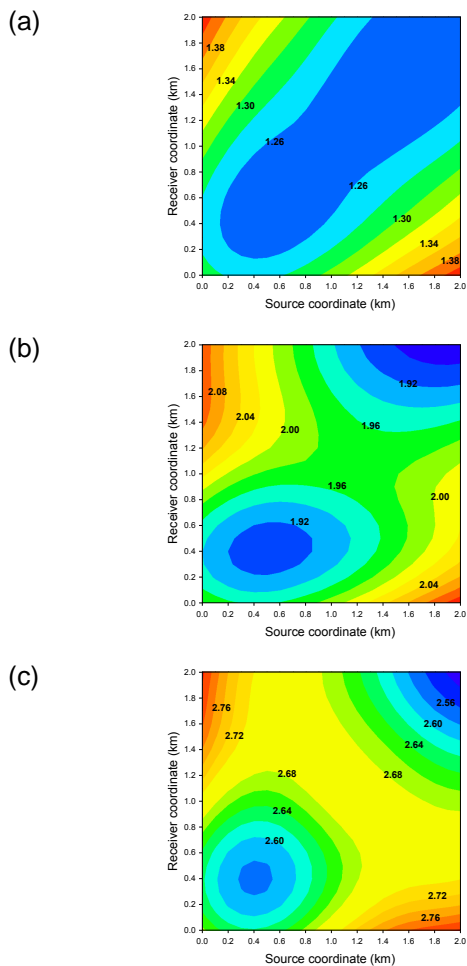


Figure 4: Simulated traveltimes (s) for waves reflected at the lowermost interface: (a) PP-wave, (b) PS-wave, and (c) SS-wave.

computed using the traveltimes in the corresponding subfigures of Figure 4. The simulated “true” SS-wave relative geometric spreading in Figure 5c is used below for comparison with the estimated results obtained using the extended “PP+PS=SS” method. The simulated relative geometric spreading for the PP- and PS-waves are not used in this method, but the two plots nevertheless serve to indicate the stability of the second-derivatives of the observed PP- and PS-traveltime functions.

In order to get an impression of the robustness of the extended “PP+PS=SS” method, we added Gaussian noise with a standard deviation of 2 ms to the input data, i.e., the PP- and PS-traveltimes in Figures 4a and 4b. For this noise level, the inherent smoothing provided by the B-spline representation was not sufficient to ensure stable calculation of second derivatives. Therefore, we introduced additional smoothing in the form of a repeated application of a Hamming operator, applied independently to the various coordinate directions. This Hamming operator smoothing is constrained by a certain aperture, defined as the maximum distance within which a given data sample will contribute to the smoothing of neighboring samples. Figure 6 shows the estimated virtual source and receiver positions for the

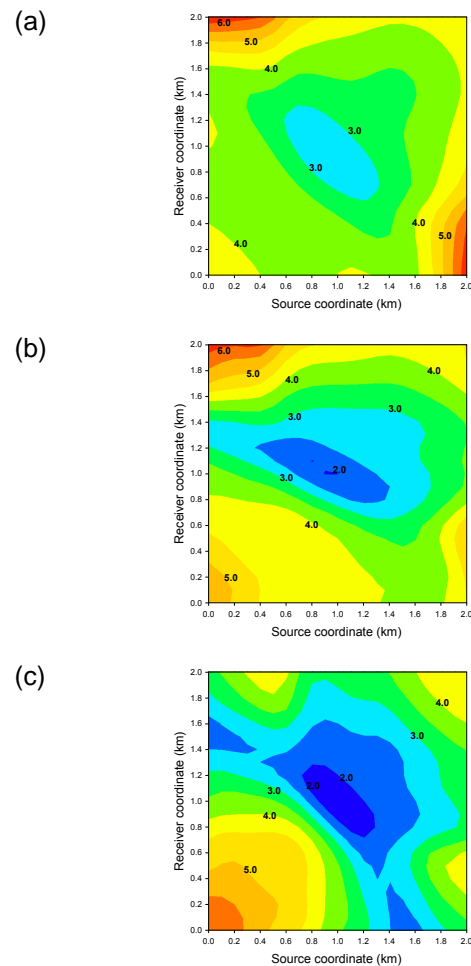


Figure 5: Simulated relative geometric spreading data (km^2/s) for waves reflected at the lowermost interface: (a) PP-wave, (b) PS-wave, and (c) SS-wave.

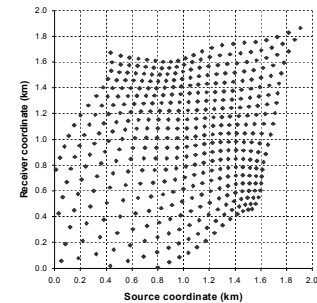


Figure 6: Reconstructed SS-wave source-receiver pairs obtained by slope matching on PP- and PS-traveltime input data containing noise. Aperture of Hamming-operator smoothing is 0.8 km.

SS-wave using a Hamming operator smoothing with aperture 0.8 km prior to the slope matching process. Using Hamming operator smoothing with aperture 0.8 km on the noisy input traveltimes data, we obtained the SS-traveltimes of Figure 7 and geometric spreadings of Figure 8. The mean errors are 0.08 % in traveltimes and 0.6 % in relative geometric spreading, while the corresponding standard deviations are 0.46 % and 12.3 %.

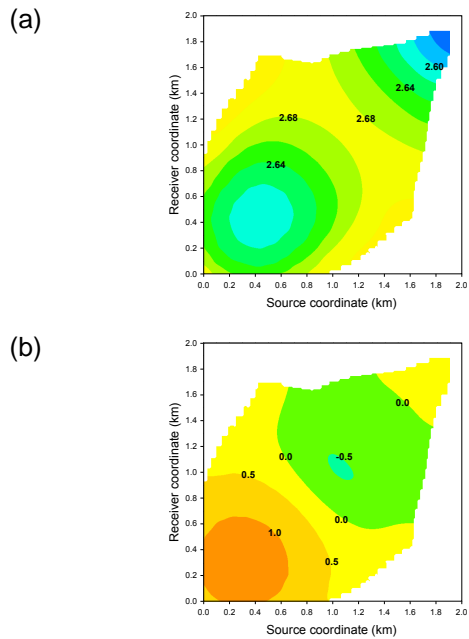


Figure 7: a) Estimated SS-wave traveltime (s), for PP- and PS-traveltime input data containing noise. Applied Hamming-operator smoothing aperture: 0.8 km. (b) Error in estimated SS-wave traveltime (%). Mean value: 0.08 %. Standard deviation: 0.46 %.

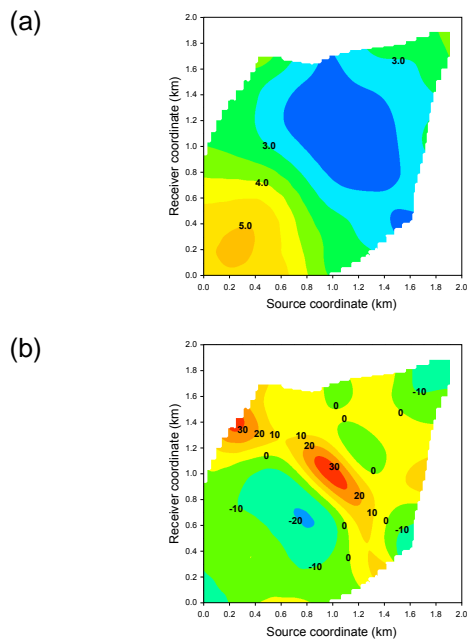


Figure 8: (a) Estimated SS-wave relative geometric spreading (km^2/s), for PP- and PS-traveltime input data containing noise. Applied Hamming-operator smoothing aperture: 0.8 km. (b) Error in estimated SS-wave relative geometric spreading (%). Mean value: 0.6 %. Standard deviation: 12.3 %.

CONCLUSIONS

For a given target reflector, the full surface-to-surface propagator matrix of an SS-wave can be obtained from the corresponding surface-to-surface propagator matrices of the PP- and PS-waves of the same reflector. This new result, which captures the second-order derivatives of SS-wave traveltime, extends the counterpart scheme of retrieving the SS-wave traveltime and slope, known in the literature as the “PP+PS=SS” method. The knowledge of the second-order derivatives of the SS-traveltime permits to determine, besides the relative geometric spreading, also the common-source and common-receiver traveltime curvatures of the SS-wave. In the same way as for PP-waves, these quantities represent useful constraints for the construction of a seismic velocity model by means of tomographic methods. Our investigation showed, however, that the proposed approach cannot provide the full amplitude of the SS-wave. The reason is the the SS-wave reflection and transmission coefficients are impossible to be retrieved from the PP- and PS-amplitudes only.

Acknowledgments

We acknowledge support by VISTA, the *Research Council of Norway* via the ROSE project, NORSAR's SIP project 181688/I30, the *National Council of Scientific and Technological Development (CNPq)*, Brazil and the sponsors of the *Wave Inversion Technology (WIT) Consortium*.

References

- Bortfeld, R., 1989, Geometrical ray theory: Rays and traveltimes in seismic systems (second-order approximations of the traveltimes): *Geophysics*, **54**, 342–349.
- Červený, V., 2001, *Seismic ray theory*. Cambridge University Press.
- Duveneck, E., 2004, 3D tomographic velocity model estimation with kinematic wavefield attributes: *Geophysical Prospecting*, **52**, 535–545.
- Foss, S.-K., B. Ursin, and M. de Hoop, 2005, Depth-consistent reflection tomography using PP and PS seismic data: *Geophysics*, **70**, U51–U65.
- Grechka, V. and I. Tsvankin, 2002, PP + PS = SS: *Geophysics*, **67**, 1961–1971.
- Hubral, P., 1983, Computing true amplitude reflections in a laterally inhomogeneous earth: *Geophysics*, **48**, 1051–1062.
- Iversen, E., 2006, Amplitude, Fresnel zone and NMO velocity for PP and SS normal-incidence reflections: *Geophysics*, **71**, W1 – W14.
- Iversen, E. and H. Gjøystdal, 1984, Three-dimensional velocity inversion by use of kinematic and dynamic ray tracing: *Society of Exploration Geophysicists, 54th Annual International Meeting*, 643–645.
- Schleicher, J., M. Tygel, and P. Hubral, 1993, Parabolic and hyperbolic paraxial two-point traveltimes in 3D media: *Geophysical Prospecting*, **41**, 495–513.
- Thomsen, L., 1986, Weak elastic anisotropy: *Geophysics*, **51**, 1954–1966.
- Ursin, B., 1982, Quadratic wavefront and traveltime approximations in inhomogeneous layered media with curved interfaces: *Geophysics*, **47**, 1012–1021.